

Impact of Geological Heterogeneity on Early-Stage CO₂-Plume Migration: Sensitivity Study

Meisam Ashraf

Knut-Andreas Lie

Halvor M. Nilsen

Arne Skorstad

October 22, 2013

1 Introduction

Sedimentary basins consist of thick piles of lithified sediments that provide large volumes that can be used to store carbon dioxide produced from localized sources as a possible means to reduce the rate of anthropogenic emission into the atmosphere [25, 18]. Sedimentary basins contain fluids (mostly brine) whose flow is controlled by high-permeable strata through which the fluids can flow and low-permeable strata which inhibit fluid flow. How efficient the geological storage of CO₂ will be, is determined by how the low and high permeability strata are stacked inside the sedimentary basin [24]. Carbon dioxide injected deep in a sedimentary basin will form a plume that has a lower density than the formation brine and hence will migrate upward by buoyancy forces. The most secure type of geological storage is therefore provided in depleted petroleum reservoirs that contain stratigraphic and structural traps that have held hydrocarbons for million of years. Unfortunately, oil and gas reservoirs do not contain sufficient pore volumes to store the large amounts of CO₂ that are required to significantly reduce current and future carbon emissions. A more viable solution is to use saline aquifers that have very slow flow rates and offer large volumes of pore space. Aquifers are typically connected to the surface through permeable strata, and the injected CO₂ may therefore in principle travel in the up-dip direction and eventually leak out through sedimentary outcrops. In practice, this process will take millions of years because of the long distances involved. Moreover, as the plume migrates upward, some of the CO₂ will be trapped as small droplets between rock grains (residual trapping), some of it will dissolve into the formation water (dissolution trapping), and some of it will react with rock minerals and become permanently trapped. In general, the flow of CO₂ in subsurface rocks is governed very complex interactions between physical forces acting on the reservoir fluids and properties of the reservoir rock itself. It is therefore necessary to develop effective (numerical) models that can be used to accurately describe the pertinent flow dynamics and provide a detailed inventory of injected volumes. Numerical models must also properly account for geological heterogeneity—i.e., variations in hydraulic conductivity and fluid storage—and how this heterogeneity influences the flow dynamics.

The main concern for policy makers and the general public is the operational safety and the risk of leakage, i.e., how likely it is that the injected carbon dioxide (or highly saline brine) will migrate into water resources, into active petroleum reservoirs, or back to the surface through ill-plugged wells [43], through caprocks broken by the high pressure imposed to the system during the injection operation, or via conductive features like fractures and faults. Likewise, there is a concern about pressure buildup, which may extend much further than the injected CO₂ plume (the effluent of CO₂ into brine). In other words, the operator of a potential injection site needs to maximize storage volumes while minimizing leakage risks and effects on areas surrounding the injection point. Over the last two decades, there have been a large number of simulation studies of CO₂ sequestration, including in particular, studies of pilot projects like Sleipner [13, 7, 12, 40, 9], In Salah [8, 11, 46], Ketzin [21, 34, 29, 30, 45], or Johansen [2, 6, 19, 17, 52]).

Geological heterogeneity is recognized in many studies as a major control mechanism that influences flow from small laminated scales to large global scales. Stratigraphic heterogeneity, for instance, is dependent on the depositional environment, and affects the geometry and spatial distribution of depositional facies as well as the spatial permeability distribution within facies. Practically, including all details of every scale into flow simulation model is impossible. Moreover, the understanding of the geology of a specific reservoir or aquifer is typically (surprisingly) limited: experience from the

petroleum industry shows that drilling new wells into mature reservoirs typically reveal structural and stratigraphic details that were not visible in state-of-the-art 3D/4D seismic surveys. The description of the geological heterogeneity will therefore have large uncertainties attached. Deep saline aquifers that have been identified as potential storage sites are typically much less characterized: the aquifer has typically been penetrated by a small number of wells, if any, and 3D seismic surveys often have limited coverage. If flow simulations are to be used to assess risks associated with a storage operation, the numerical flow model must properly account for the impact of uncertainty in the geological description. Yet, most studies of CO₂ injection commonly employ simplified or conceptualized reservoir descriptions, in which the medium is considered (nearly) homogeneous, or use a single petrophysical realization, and instead focus on developing complex models of the flow physics, discretization schemes, and solvers.

Early studies of the impact of heterogeneity consider 2D models with geostatistically populated permeabilities [33, 51]. Likewise, a layered heterogeneity is examined in [37]. Later, Hovorka et al. [26] studied the impact of heterogeneities in the Frio formation from the Texas Gulf Coast, including stratigraphic heterogeneities resulting from transitions between rocks deposited in sand and mud-dominated depositional facies and structural heterogeneity from growth faults, folds, and salt diapirs. The heterogeneities were parametrized and used as input to a solver to assess the effectiveness of CO₂ storage and its sensitivity to these parameters. Likewise, Obi and Blunt [44] investigate the heterogeneity in an oil field in the North Sea including fluvial and a prograding depositional environment. Flett et al. [20] constructed a suite of 3D models, in which a radial variogram was used to populate five models with varying net-to-gross ratios, and concluded that formations containing shale barriers are effective in containing an injected CO₂ plume within the formation and that heterogeneity serves to limit the reliance of the formation seal as the only mechanism for containment. Nilsen et al. [41, 50] considered a large set of high-resolution models of the top surface and concluded that uncertainty in morphology effects at a small scale may have a significant impact on (large-scale) estimates of the non-trivial interplay between structural and residual trapping. The opposite case, with a single top-surface topology and multiple property realizations, was considered by Goater et al. [23].

The most comprehensive study geological uncertainty to day, however, was conducted in the SAIGUP project, which focused on how geological uncertainty impacts reserve estimates and production forecasts [38, 27, 39]. Here, an ensemble of synthetic but realistic models of shallow-marine reservoirs were generated and several thousand cases were run for different production scenarios. The results showed that realistic variations in the structural and sedimentological description have a strong influence on production responses. In general, one cannot expect that knowledge of how geological heterogeneity impacts flow predictions of oil-water systems can be carried directly over to CO₂-brine systems relevant for CO₂ injection scenarios, which involve temporal and spatial scales and density ratios that are quite different from those encountered in oil recovery. Potential storage sites may also have geological characteristics that differ from those seen in producible oil reservoirs. Nevertheless, we will herein try to leverage the comprehensive geomodeling effort from SAIGUP. To this end, we consider a scenario in which CO₂ is injected into an abandoned shallow-marine reservoir and use geological realizations generated as part of the SAIGUP project—which, geologically speaking, represent a viable storage site—to study the impact of geological heterogeneity on the short to medium term predictive modeling of CO₂ plume formation and migration. How heterogeneity impacts the injection operation will be studied in a separate work, in which we also discuss more realistic pressure constraints on injection well.

The outline of the paper is as follows: We start by describing the geological realizations, the underlying parameters, and the flow model in Section 2. In Section 3, we introduce a set of flow responses that we will use to describe the feasibility of the storage operation and the variations in the resulting flow patterns. Section 4 analyzes how the various geological parameters impact the formation and early-stage migration of the CO₂plume. In Section 5, we discuss how the contact between the CO₂ plume(s) and the caprock, and hence the leakage risk, is influenced by the geological parameters. Finally, some concluding remarks are given in Section 6.

2 Model Setup

Sedimentary basins are formed by superposition of high and low permeable strata that control the lateral and vertical flow of the fluids in the medium. Aquifers consist of layers with high permeability and therefore usually have pressure distributions that are (almost) hydrostatic. Lower-permeable parts of the basin are called aquitards, and here the flow will be orders of magnitude slower than in aquifers. However, the area exposed to flow may be very large, which consequently enables large volumes to flow across bedding between two adjacent aquifers. Aquifers and aquitards can be covered by evaporitic beds that are almost impermeable (aquiclude) [24].

The flow in aquifers generally depend on the balance between viscous, capillarity, and segregation forces. Viscous forces act because of the pressure change imposed by wells or background flow within the medium. In regions with slow velocities, capillary forces will dominate and in high permeability regions, gravity segregation can be considerably dominant. Any of these forces can be important for the movement of the injected CO₂. Herein, we consider the injection and early migration phase for a storage operation in which supercritical CO₂ is injected into a shallow-marine reservoir underneath a sealing cap-rock that forms a type of structural trap that is often seen in petroleum reservoirs. This means that we can expect viscous dominance during injection and gravity dominance during the subsequent migration phase.

To represent the aquifer geology, we use an ensemble of synthetic models developed in the SAIGUP study [38]. The SAIGUP models were originally designed to encompass the sedimentological architectures and fault structures of European clastic oil reservoirs, with a focus on shoreface reservoirs. Here, the deposition of sediments is due to variations in sea levels so that facies are forming belts in systematic patterns (curved belts for river deposits, parallel belts for wave deposits, etc). Sediments are deposited when the sea level is increasing, whereas barriers may be formed when the sea level is decreasing. Shoreface reservoirs are bounded by faults and geological horizons.

To derive an objective geological parametrization, the SAIGUP project indexed a broad suite of shallow-marine reservoir to continuously varying anisotropy and heterogeneity levels, structural complexity ranges from unfaulted to compartmentalized, and fault types from transmissive to sealing. From this, a set of geological realizations were created with sedimentary heterogeneity changing in different levels of heterogeneity in lateral and vertical directions. Structural heterogeneity was represented by variations of the fault orientations, intensity, and the transmissibility across the fault. Particular care was taken to ensure that the number of realizations was sufficient to form a basis for sensitivity analysis and that there was enough overlap in the geological parameter variations between realizations to allow for quantitative assessment of the contribution of each geological parameter. Although models are synthetic, each realization should be complex enough to represent a plausible geology suitable for realistic flow modeling.

The geological realizations were built within a sequence stratigraphic framework for progradational shallow-marine sedimentary environments. A regular grid was used to model the sedimentological parameters, with structural modeling added to the models afterwards. The depositional modeling started by population of six facies associations, each with internal heterogeneity on a fine grid. Lamina-scale models (meter-scale) were built to capture the lamina-scale effects on flow through each facies. Some of these facies were modeled in three dimensions to account for anisotropy; some were modeled deterministically, while other facies were populated stochastically. Figure 1 shows an illustration of the modeled facies for a specific case. Next, the facies produced at appropriate lamina scales were upscaled by geo-pseudo methods in different intermediate steps and finally mapped onto a geological grid. This grid was considered too fine for the flow simulation and was upscaled in a last step to a coarse grid (Figure 2). Each grid-block in the coarse simulation model were represented by values of porosity, net-to-gross ratio (shale content), directional permeabilities, and an index to the facies contained in the grid-block. Specifications of the fine and coarse grids are given in Table 1.

In our study, we have selected the following five parameters that altogether give 160 realizations:

Lobosity – is defined by the plan-view shape of the shoreline. As a varying parameter, lobosity indicates the level at which the shallow-marine system is dominated by each of the main depositional processes. Two depositional processes are considered in the SAIGUP study: fluvial and wave processes. The higher the amount of sediment supply provided from rivers is relative to the available accommodation space in the shallow sea, the more fluvial dominant the process

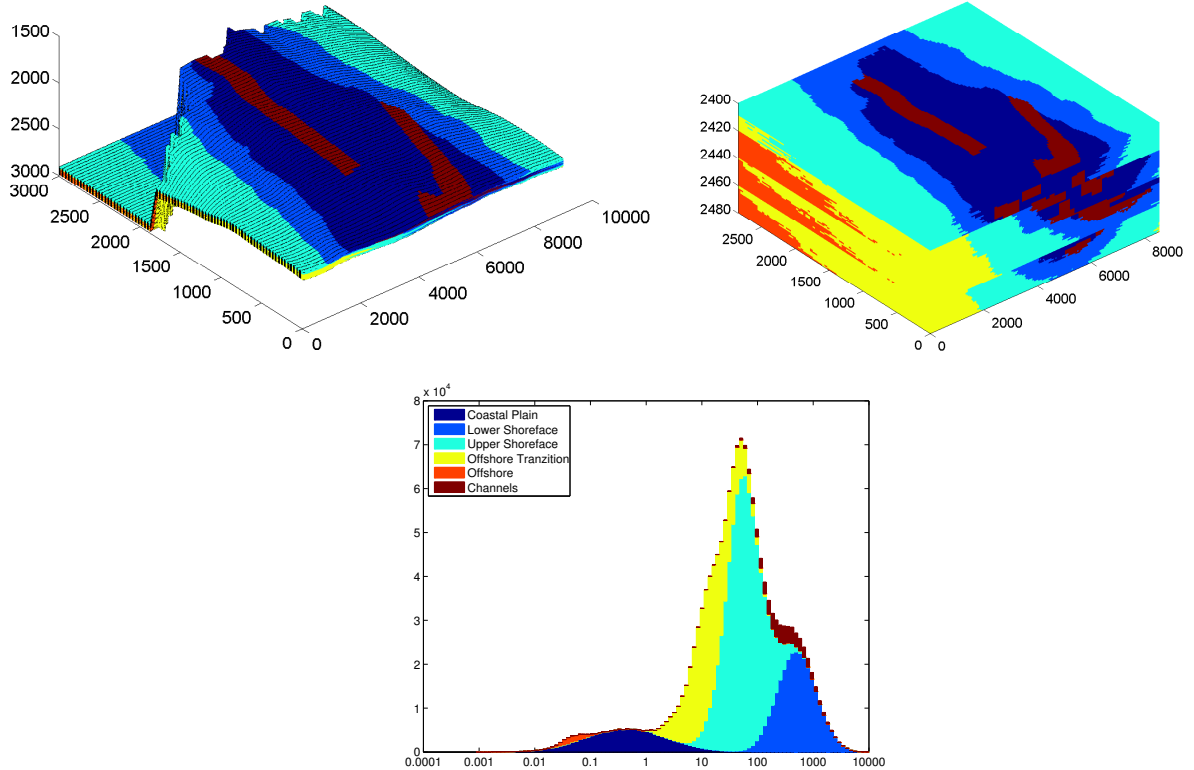


Figure 1: Facies variations for a selected fine model, with colors corresponding to different rock types. The upper-left plot shows a perspective view of the actual grid, whereas the rock types have been mapped to a uniform grid for a better visualization to the upper right. The lower plot shows a histogram of the logarithm of the lateral permeability (unit: $\text{cP m}^3/\text{day}/\text{bar}$).

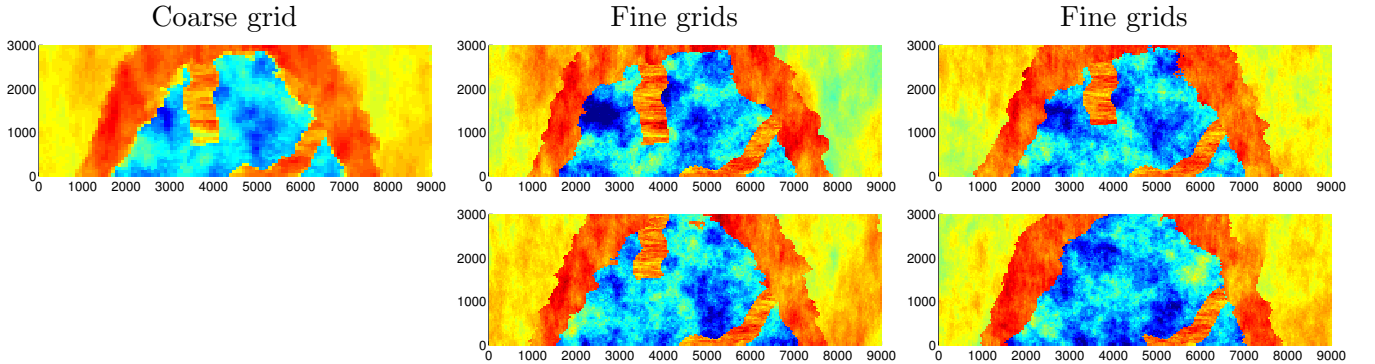


Figure 2: Top view of the logarithm of the lateral permeability plotted for the first four layers of the fine grid versus their representative layer in the coarse grid.

Table 1: Specifications for the fine and coarse grids used in the SAIGUP modeling process.

Parameter	Fine scale	Coarse scale
Grid spacing (x -direction)	37.5 m	75 m
Grid spacing (y -direction)	37.5 m	75 m
Grid spacing (z -direction)	1 m	4 m
Total number of cells	1,500,000	96,000
Number of active cells	1,500,000	79,000
Lateral extent (x -direction)	6 km	6 km
Lateral extent (y -direction)	9 km	9 km
Vertical extent (z -direction)	80 m	80 m

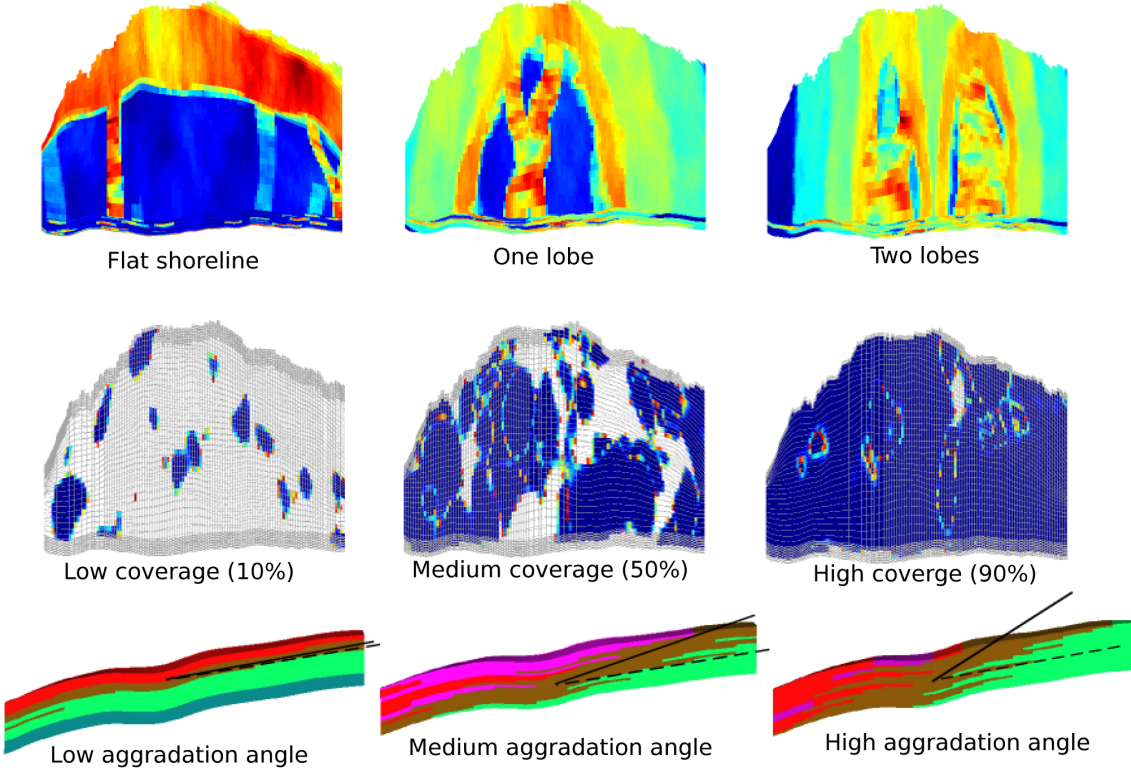


Figure 3: Illustration of geological parameters from the SAIGUP study: the top row shows three different lobosities for up-dip progradation (if the lobes flip over the long axis, we will have down-dip progradation); the middle row shows barriers representing different degrees of mud-draped coverage; and the bottom row shows aggradational angle.

will be. As the river enters the mouth of the sea, it can divide into different lobes and branches. Wave processes from the sea-side smear this effect and flatten the shoreline shape. Less wave effect produces more pronounced lobe shapes around the river mouths. Very high permeability and porosity can be found in the channeling branches, while dense rock with low permeability fills the space between them. Reservoir quality decreases with distance from the shore-face. We expect that the level of lobosity can have a considerable effect on the CO₂ injection and plume size in the aquifer. Models of three levels of lobosity are used herein: flat shoreline, one lobe, and two lobes, as illustrated in the upper row of Figure 3.

Barriers – Periodic floods result in a sheet of sandstone that dips, thins, and fines in a seaward direction. In the lower front, thin sheets of sandstone are interbedded with mud-stones deposited from suspension. These mud-draped surfaces will potentially act as significant barriers to both horizontal and vertical flow, and are modeled by transmissibility multipliers corresponding to three levels of coverage for the barrier sheet: low (10%), medium (50%), and high (90%), as illustrated in the middle row of Figure 3.

Aggradational angle – In shallow-marine systems, two main factors control the shape of the transition zone between river and basin: amount of deposition supplied by the river and the accommodation space that the sea provides for these depositional masses. One can imagine a constant situation in which the river is entering the sea and the flow slows down until stagnation. The deposition happens in a spectrum from larger grains depositing at the river mouth to fine deposits in the deep basin. If the river flux or sea level fluctuates, the equilibrium changes into a new bedding shape based on the balance of these factors. The SAIGUP data models cases in which, for instance, the river flux increases and shifts the whole depositional system into the sea. The angle at which the transitional deposits are stacked on each-other because of this shifting, is called aggradational angle. Three levels of aggradational angle are modeled here: low, medium, and high angles. The three parameter choices are illustrated in the bottom row of Figure 3, where we in particular notice how a low aggradational angle gives continuous facies layering parallel to the dip

Table 2: Geological parameters from the SAIGUP project included in this study. The last column reports markers used to distinguish different parameters in the plots.

Parameter	Levels	Marker
Lobosity	flat, one-lobe, two-lobe	square, circle, diamond
Barrier	low(10%), medium(50%), high(90%)	small, medium, large
Aggradation	low(parallel layering), medium, high	blue, green, red
Progradation	up-dip, down-dip	first half, second half
Fault	unfaulted, open faults, closed faults	thin, medium, thick

direction of the model.

Progradation – denotes the direction of the depositional dip. Two types are considered here: up and down the dominant structural dip. Because the model is tilted a little, this corresponds to the lobe direction from flank to crest or vice versa.

Fault – are represented by three different parameters in the SAIGUP study: fault type, intensity, and transmissibility. Herein, we limit our study to compartment faults of medium intensity and consider three parameter choices: no faults, open faults, and closed faults.

Table 2 lists the markers (shape, size, color, thickness) that will be used to signify different parameter values in plots of simulation results later in the paper.

We will consider storage of forty million cubic meters of supercritical CO₂, which amounts to approximately 20% of the total pore volume in the aquifer. The CO₂ will be injected from a single well over a period of thirty years, and after the injection period, seventy years of plume migration is simulated for all cases. Hydrostatic boundary conditions are imposed on the sides, except at the faulted side on the crest, and no-flow boundary conditions are imposed on the top and bottom surfaces.

If the medium was homogeneous and of sufficient permeability, one would expect that the injection would create one big plume that moves upward because of the gravity force until it accumulates under the structural trap of the cap-rock, i.e., migrating from the injection point and upward to the crest of the aquifer. The idea is therefore to inject as deep as possible to increase the travel path and the volume swept by the plume before it reaches the crest. To this end, the injector is placed down in the flank and only completed in the three lowest layers of the aquifer. The formation and early migration of the plume will crucially depend on the complex interaction between the injected CO₂ and the heterogeneity inside the reservoir; that is, whether the CO₂ encounters low permeability rocks in the vicinity of the well bore, or whether high permeability pathways are available to enable plume migration away from the injection point. The fixed well position was chosen manually based on a number preprocessing simulation runs and held fixed for all model realizations. This way, we avoid introducing an additional parameter into the simulation study. On the other hand, we may also introduce certain artifacts, like exaggerated pressure responses if the well hits a low-permeable area, that would have been avoided if the well position was optimized for each realization. A more comprehensive study should, of course, also have investigated possible effects and impacts of different well positions and completion strategies to increase the robustness of the observations.

The injected CO₂ is assumed to be a supercritical fluid with density 700 kg/m³ and viscosity 0.04 cP. The supercritical fluid is modeled as a dead oil with a formation factor of 1.1 at 0 bar and 0.95 at 400 bar. (The assumption of (almost) constant properties is reasonable since pressure and temperature effects will typically counteract each other at relevant depth ranges.) Brine is assumed to be slightly compressible ($3.03 \cdot 10^{-6}$ psi⁻¹) with density 1033 kg/m³ and viscosity 0.4 cP. The rock compressibility is set to $3 \cdot 10^{-7}$. For both fluids, we will use Corey-type relative permeability functions

$$k_{rCO_2} = (1 - S)^\alpha, \quad k_{rw} = S^\alpha, \quad \alpha = 1, 2$$

where S denotes the saturation of brine normalized for end points 0.2 and 0.8.

Relative permeabilities for CO₂-brine systems have been thoroughly discussed in the literature; [4, 5, 22] summarize 35 experiments on sandstone and carbonate rocks and more experiments can be found in [1, 47, 53]. There are also papers that analyze the impact of the relative permeability (e.g., [10, 31, 32]), and investigate the endpoint and hysteresis effects, see e.g., [49, 28]. In many

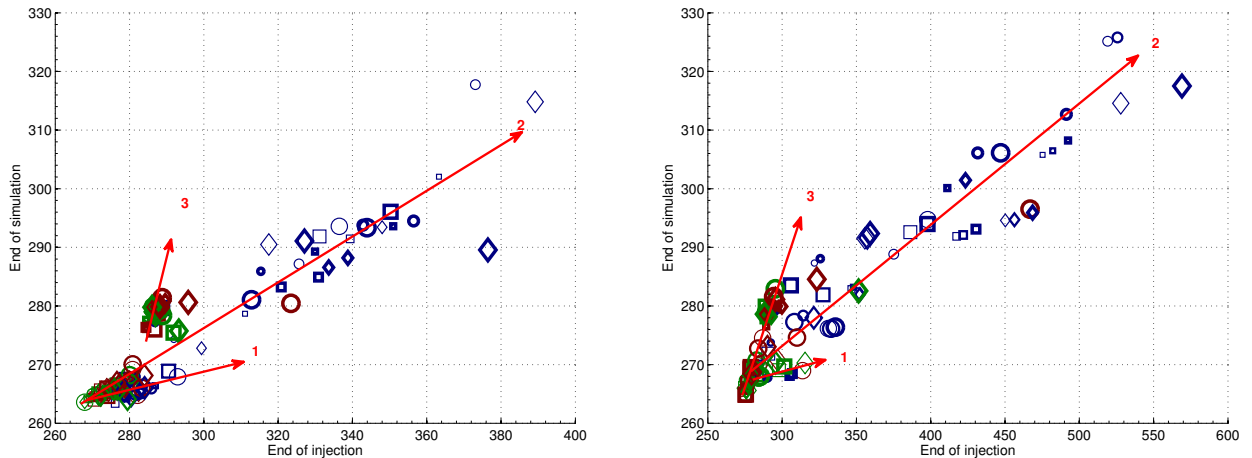


Figure 4: Cross-plot of average aquifer pressure at the end of simulation versus at the end of injection for linear (left) and quadratic (right) relative permeabilities.

storage scenarios, however, the segregation of supercritical CO₂ and brine will typically take place in the rock with high permeability. This is the basis for the popularity of so-called vertical-equilibrium models [42] for investigating CO₂ sequestration. The effective relative permeability after segregation has occurred is linear if capillary effects are small, and if nonlinear relative permeabilities are used, large errors will occur in cells in which segregation should have occurred and the saturation is low, as demonstrated in [36]. Sensitivity to vertical grid resolution is also observed by Wei and Saaf [52]. In the following, we will therefore primarily use linear relative permeabilities, even though this choice is not necessarily representative on the small scale. Introducing linear relative permeabilities can be viewed as using the pseudo-relative permeabilities that are least influenced by the vertical grid resolution and best represent the flow of the system for large grid blocks. In addition, using linear relative permeabilities not only simplifies and speeds up the flow simulations, but also accentuates and accelerates the flow effects we study. For completeness, however, we also report results using nonlinear relative permeabilities.

3 Basic Flow Responses

In this section we will give a qualitative discussion of how some basic flow responses like the wave speeds of the plume migration, average aquifer pressure, mobile and residually trapped volumes, and plume sizes are affected by variations in the geological parameters.

3.1 Pressure responses

The average aquifer pressure in general shows a sharp jump at the start of injection and a declining trend during injection and plume migration caused by pressure release through the open boundaries. (Specifying different boundary conditions would have resulted in different pressure trends). Figure 4 shows cross-plots of the average aquifer pressure at the end of injection and end of simulation for our two different choices of relative permeability functions. In both plots, one can recognize three different trends which have been indicated by three straight lines. The first trend, which has the gentlest slope, represents cases with large pressure variation during injection and small range of pressure variation during the migration phase after the end of injection. In these cases, the heterogeneity of the medium forms channels toward the open boundaries through which the injection pressure is released, resulting in low aquifer pressure at the end of simulation. The second trend, represents cases in which the heterogeneity affects injection, gravity segregation, and flow through open boundaries. In particular, we observe that most cases that have high injection pressure correspond to a low aggradational angle, for which low vertical permeability forces the injected CO₂ plume to move relatively slow in the lowest, poor-quality layers before migrating up toward the cap-rock, see Figure 5. This increases the pressure in the domain during injection and keeps a higher pressure gradient to the open boundaries. In the third trend, which includes scenarios with closed faults, the heterogeneity makes chambers and

Table 3: Geological parameters for four different cases selected for visualization.

Case	Faulted	Lobosity	Barrier	Aggradation	Progradation
Case 1	no	one-lobe	medium	medium	down-dip
Case 2	no	two-lobe	medium	low	up-dip
Case 3	no	one-lobe	high	high	up-dip
Case 4	no	one-lobe	high	high	down-dip

compartments in which the pressure increases during injection and then remains high. Heterogeneity also affects the gravity segregation process more than in the other two trends because of faults and a high barrier coverage.

We also see the effect of curvature in the relative permeabilities by comparing the two plots in Figure 4. Higher range of pressure variations is observed during injection for the nonlinear relative permeability runs. Moreover, nonlinear relative permeability gives lower mobility which leads to higher pressure build-up during injection. This means that longer time is required for the pressure to be released through the open boundaries after injection and more cases therefore follow the second and third trend. More details about the bottom-hole pressure are given in a companion paper [3], which also discusses more realistic constraints on the injection operation.

3.2 Plume migration

The direction in which the CO₂ plume moves in the medium will primarily impact the amount of residual (and structural) trapping, but as we will see later, also significantly change the extent to which the plume contacts the caprock, which again affects the risk for leakage through breaches and holes in the caprock. When evaluating the safety of a long-term storage operation, there are several potentially conflicting aspects that need to be considered with regard to plume migration. On one hand, we prefer the plume to spread out laterally to enhance residual trapping and mixing of CO₂ and brine; the amount of residual trapping is positively correlated with the sweep efficiency of the CO₂ plume, i.e., the percentage of the aquifer volume that has been in contact with CO₂. On the other hand, one typically wants to confine the plume to the smallest volume possible to simplify monitoring operations, minimize the contact with potential leakage points, and minimize the risk of leakage and contamination into other aquifers. However, if a big movable plume connects with a leakage pathway through the caprock, large volumes of CO₂ may escape, and for this reason, it may be better if the injected CO₂ splits into many small plumes. To investigate these aspects, we will study the number of plumes and their volumes.

3.2.1 Boundary fluxes

Because we have chosen to inject a relatively large amount of CO₂ corresponding to one fifth of the aquifer's pore volume, it is to be expected that the pressure and saturation fields will interact strongly with the model boundaries, which in some cases will lead to substantial loss of CO₂ across the boundaries. The model has open boundaries on three sides, which are modeled by imposing huge pore-volume multipliers in the outer cells, while no-flow boundary conditions are imposed along the top faulted side. Using large pore-volume multipliers to represent open boundaries enables volumes of CO₂ to leave and later re-enter the aquifer. (In addition, this method will contribute to eliminate effects from Dirichlet type boundary conditions). The flux out of the open boundaries can be considered as a measure of the lateral movement of the plume, and reflects the relative difficulty of forcing the injected CO₂ up-dip towards the crest compared with driving it down-dip through the nearby open boundaries.

The lower boundary is closest to the injection point and hence the most likely place where injected CO₂ volumes will escape. Figure 6 shows plots of the CO₂ flow across this boundary at the end of injection versus the flow across the boundary at the end of simulation. Toward the end of injection, most cases have positive flux values, which means that parts of the main plume connected to the injection point have been forced to leave the domain in the down-dip direction by the increased injection pressure. However, after injection stops, many cases have small negative fluxes, which means that a small volume of CO₂ reenters the domain. Once again, we observe that cases with low aggradation

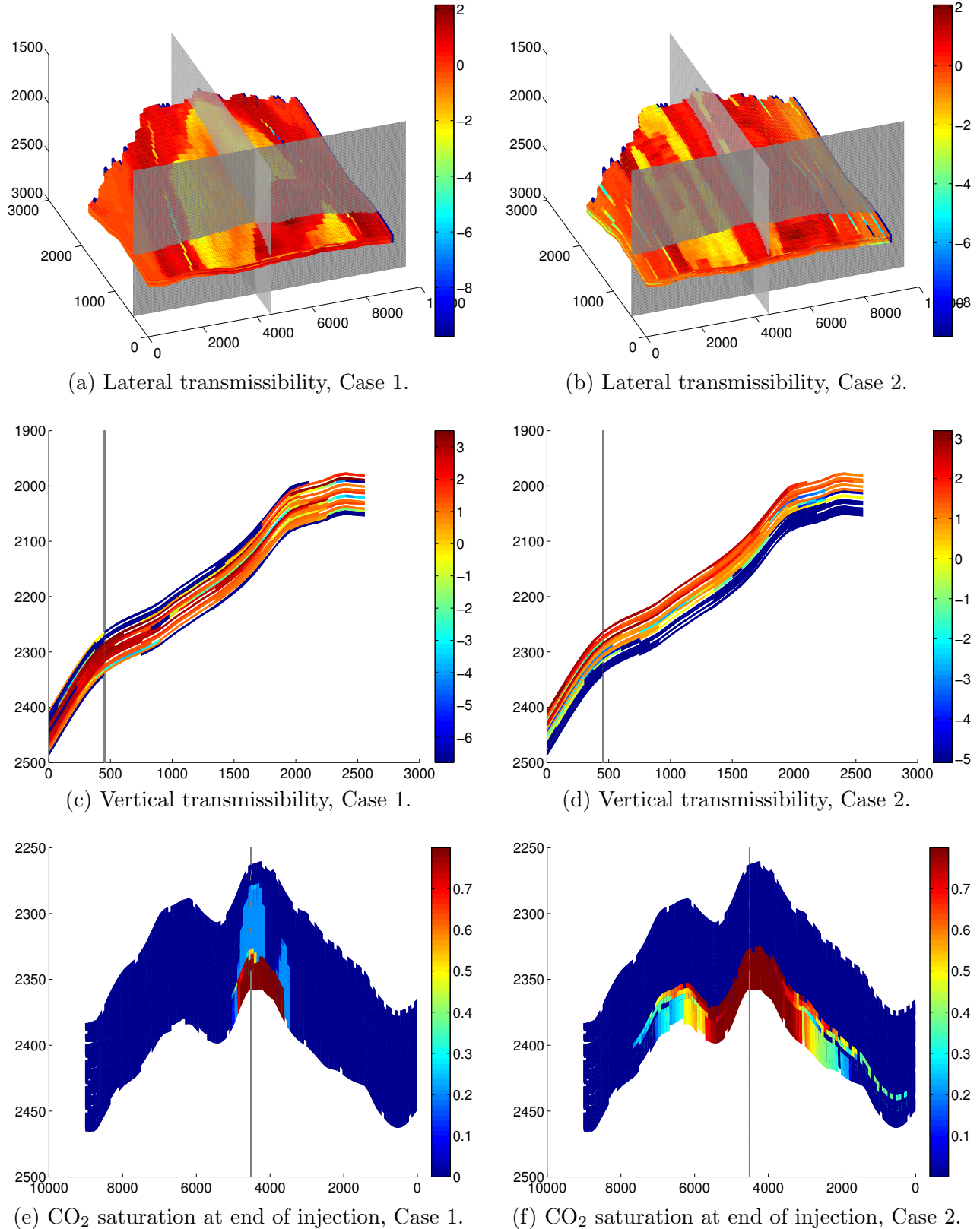


Figure 5: Impact of heterogeneity on CO_2 flow for Cases 1 and 2 in Table 3. The slice planes used to create the side views in (c) to (f) are shown as in gray in the perspective views in (a) and (b).

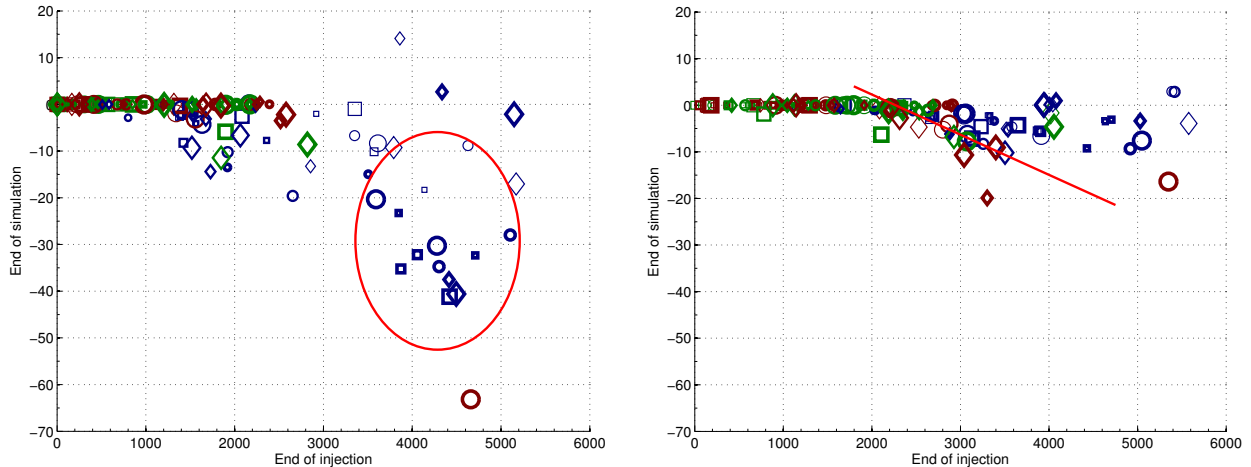


Figure 6: Cross-plot of CO₂ flux out over the down-dip boundary for linear (left) and quadratic (right) relative permeabilities. Positive values represent outward fluxes and negative values represent inward fluxes.

angle stand out from the rest. In these cases, the injected plume is almost entirely confined to the bottom of the model because of poor vertical communication (see Figures 5 and 7). Hence, a large portion of the injected volume will be forced out of the domain in the down-dip direction. After the end of injection, gravity forces will gradually cause some of these lost volumes to move up-dip again and reenter the domain. We notice that cases with closed faults (shown is the red circle in the left plot of Figure 6) show a relatively higher return flux for the linear relative permeability function. With nonlinear relative permeability function, some of the cases follow a linear trend (shown by the red line in the right-hand plot), in which the return flux is proportional to the outward flux.

3.2.2 Total mobile/residual CO₂

Residual trapping occurs when the CO₂ saturation is below the residual saturation value of 0.2. Although the residually trapped CO₂ is free to move in a molecular sense on the microscale, the corresponding bulk volume is considered immobile on the macro scale. To reduce the risk of leakage, it is therefore important to obtain an efficient volumetric sweep that will maximize the residual volumes and minimize the mobile volumes. Herein, we will define residually trapped volumes as volumes in which the CO₂ saturation is below the residual value of 0.2. Notice that with this definition, all mobile volumes (in which the saturation exceeds 0.2) will contain a residual portion of CO₂ that is not free to escape. This portion will eventually become residually trapped if the saturation of the mobile CO₂ decreases to the residual value.

Figure 9 shows cross-plots of the total residual volume at the end of injection versus the residual volume at the end of simulation. Drainage is the dominant flow process during injection. When injection ceases, the plume migration turns into a imbibition-dominated process which increases the residual trapping of CO₂. With linear relative permeability, the imbibition process takes place relatively fast and the residual volume increases significantly in the post-injection phase. Once again, low-aggradation cases form notable exceptions that have small amounts of residual trapping. The reason is primarily that significant volumes have been lost over the down-dip boundary, and secondarily that the (vertical) sweep is limited because the CO₂ plume is confined to the lower layers of the reservoir during most of the simulation time.

With quadratic relative permeabilities, the predicted migration process is significantly slower and many cases have almost the same residual volume at the end of injection and end of simulation. As already discussed on page 7, the prediction of the gravity segregation of CO₂ and brine is strongly affected by vertical grid resolution for nonlinear relative permeabilities and may severely under-predict segregation in low-saturation regions. On the other hand, the curvature of the relative permeability function does not have a considerable influence on the flow path (compare the streamline paths in Figure 10 for a selected case). Compared with the results in the left right plot of Figure 9, we therefore ultimately expect a significant increase in residual trapping before the plume settles; this prognos-

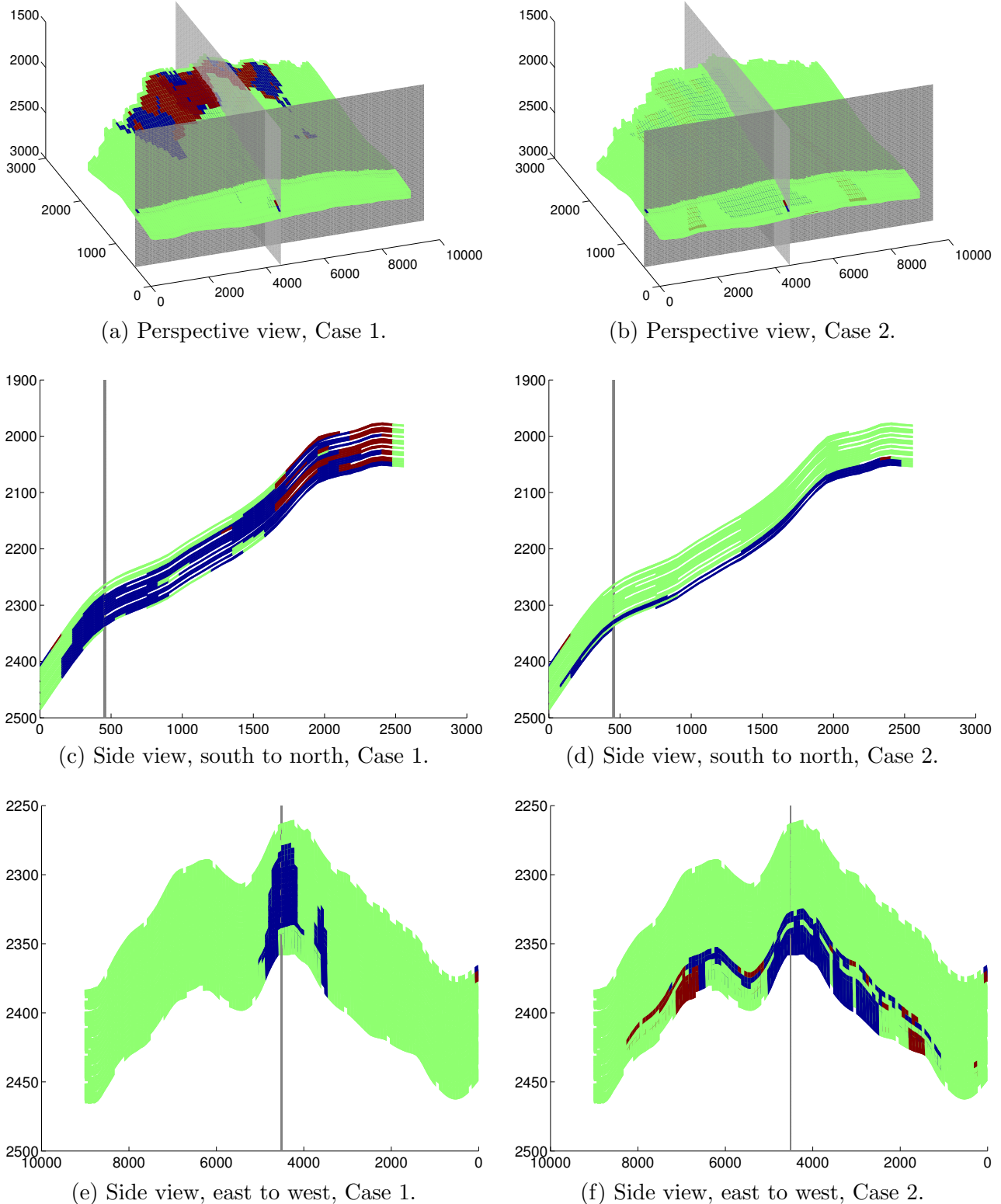
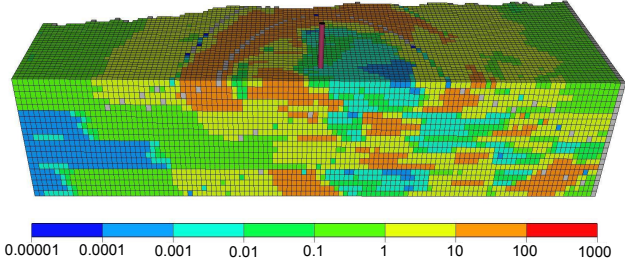
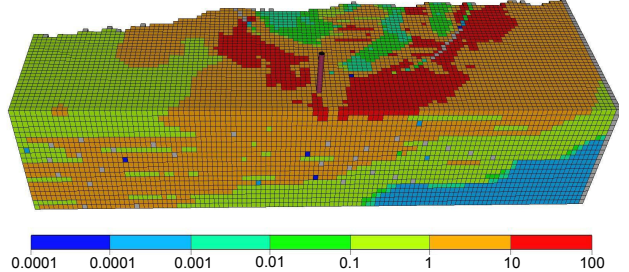


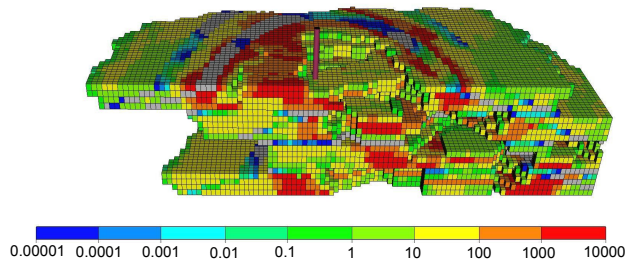
Figure 7: CO₂ flow in the dip direction at the end of simulation for Cases 1 and 2 from Table 3. Blue color shows the flow up-dip, red color the flow down-dip, and the green areas with no CO₂ flow.



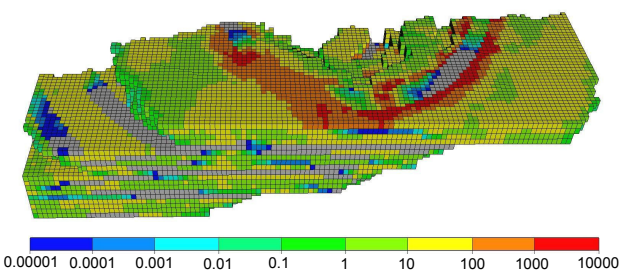
(a) Lateral transmissibility, Case 3.



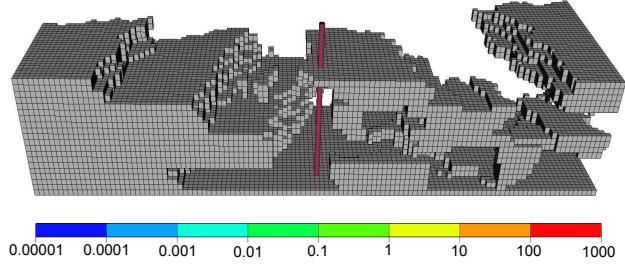
(b) Lateral transmissibility, Case 4.



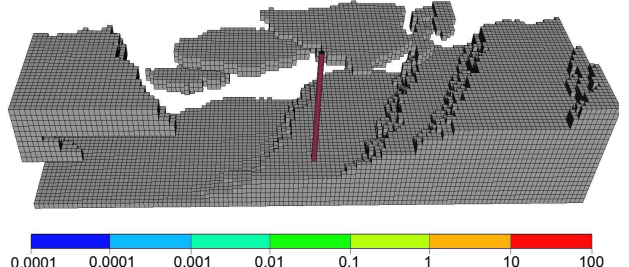
(c) Nonzero vertical transmissibility, Case 3.



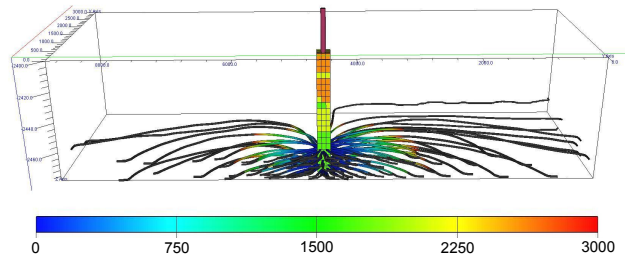
(d) Nonzero vertical transmissibility, Case 4.



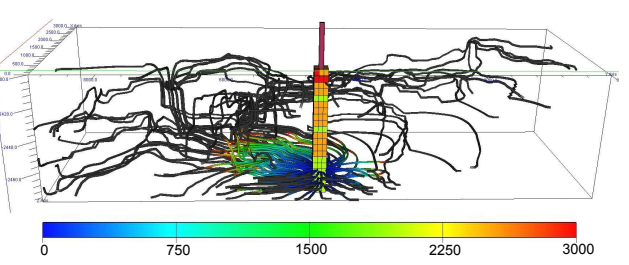
(e) Zero vertical transmissibility, Case 3.



(f) Zero vertical transmissibility, Case 4.



(g) Flow paths from injector, Case 3.



(h) Flow paths from injector, Case 4.

Figure 8: Effect of heterogeneity on CO₂ flow for Cases 3 and 4 from Table 3. The two cases differ in progradational direction, and lateral flow is enhanced in the down-dip case (Case 4).

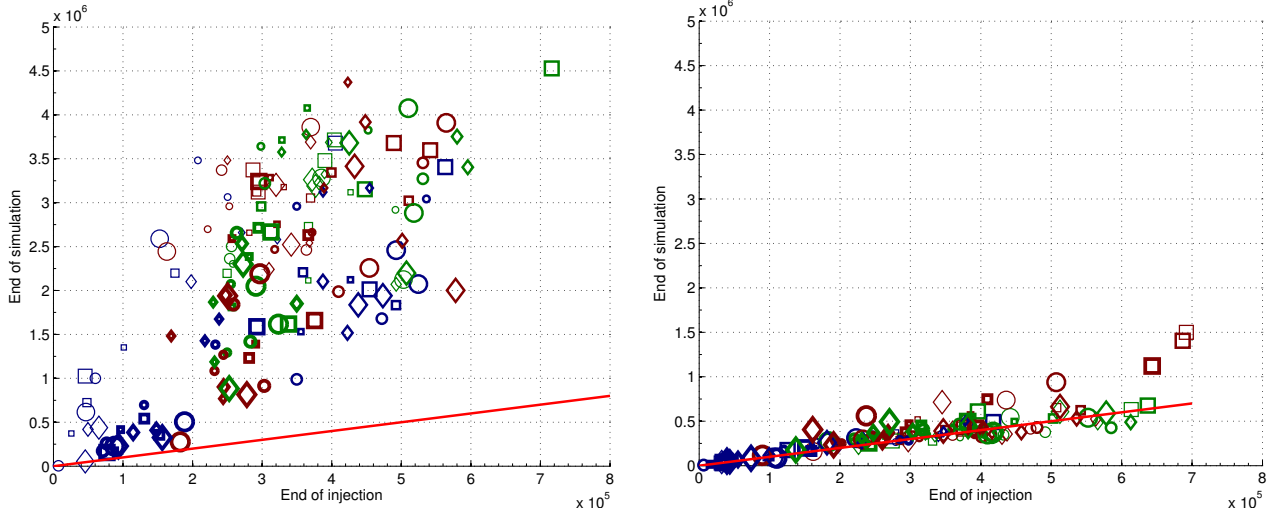


Figure 9: Residually trapped volumes for linear (left) and quadratic (right) relative permeabilities. Cases on the red lines have the same values at the end of injection and end of simulation.

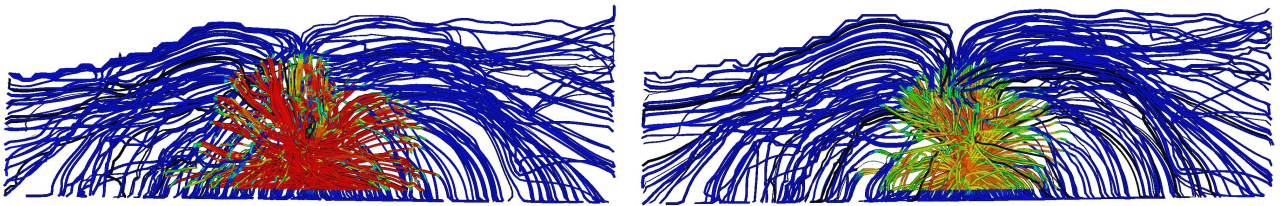


Figure 10: Top view of CO_2 saturation plotted on streamlines for linear relative permeabilities (left) and quadratic permeabilities (right). Red color corresponds to the mobile CO_2 and blue represents the water phase.

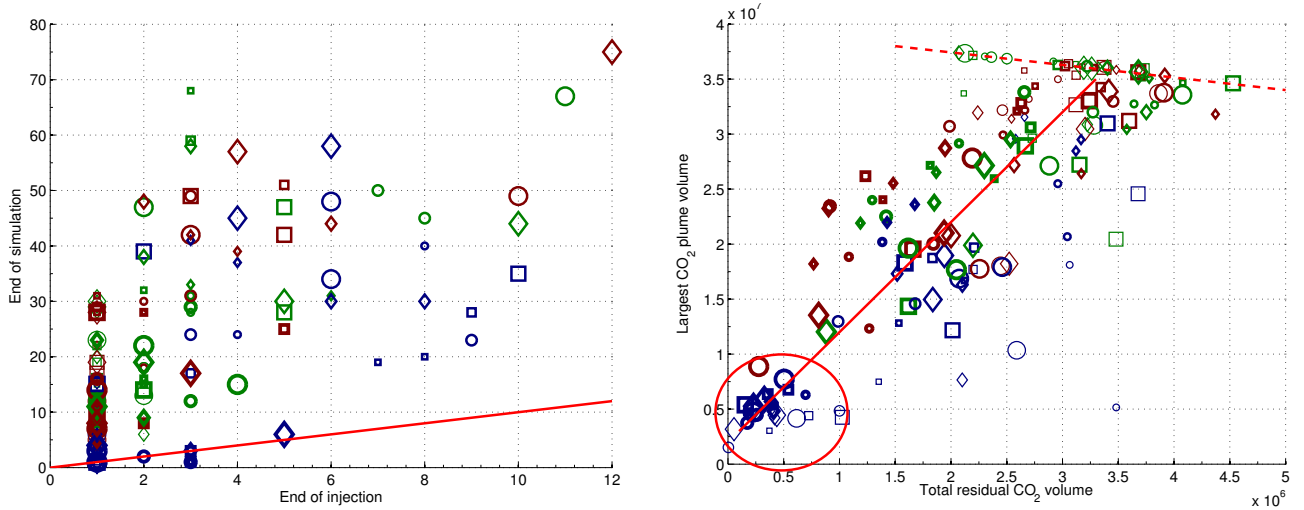


Figure 11: The cross-plot to the left shows the number of CO_2 plumes at the end of simulation versus the number of plumes at the end of injection for linear relative permeability function. The right plot shows the volume of the largest CO_2 plume versus the volume of residual CO_2 at the end of simulation.

tication has been confirmed for a few (arbitrary selected) cases by computing the plume migration for more than ten thousand years. We also observe that in some cases the residual volumes *decrease* after injection ceases. This is an artifact and is caused by mobile CO₂ invading zones of residual CO₂, thereby turning residual volumes into mobile volumes according to the definition of residual trapping used herein. These cases are therefore likely to be influenced by hysteresis effects [1, 28, 49], which for simplicity have been disregarded in this study.

3.2.3 Connected CO₂ volumes

In the next section, we will study the risk of leakage through the caprock. To this end, we will use a simplistic model which assumes that all mobile CO₂ connected to a leakage point will escape through that point. Hence, it is preferable if the total mobile CO₂ volume is split into smaller plumes rather than forming a big mobile plume. Moreover, the surface area per volume increases by splitting the plume (assuming constant plume shape) and this helps residual trapping (and mixing of brine and CO₂).

During injection, the flow support from the well builds a connected mass of CO₂ shaping one or a few big plumes. When the injection ceases, the CO₂ starts distributing in the medium and plumes may split because of branches in the flow paths created by heterogeneity. The plot to the left in Figure 11 shows how the number of plumes increases significantly in most cases during the migration phase, except for a few low-aggradation cases for which the injected plumes stay intact or reform into a single plume.

The right plot in Figure 11 shows the volume of the largest CO₂ plume versus the residual trapping. Here, we see two major trends indicated by a solid and a dashed line. The solid line, having a positive slope, represents cases that loose CO₂ through the open boundaries, mainly through the one closest to the injection point. As a consequence, less CO₂ volume exists in the system and the size of the largest plume will be smaller. Hence, less volume will be swept while the plume migrates upward (if it does), which again means that less CO₂ is residually trapped. In particular, we notice the cases inside the ellipse which are the same cases that had large CO₂ volumes escaping through the down-dip boundary as shown in Figure 6. The dashed line with negative slope corresponds to cases for which almost all of the injected CO₂ stays inside the domain. These cases show a small range of variation for the largest plume size and are reflecting the effect of different heterogeneity features on the residual trapping process. Because equal volumes of CO₂ are injected in all cases, we notice that the bigger the main plume is, the smaller the residual volume will be (mainly because the fraction of CO₂ that corresponds to saturation below 0.2 inside the movable plume is not considered to be residually trapped according to the definition used herein).

4 Analysis of Parameter Impact

The main purpose of the current study is to investigate how geological heterogeneity impacts the formation of a CO₂ plume during injection and during the early-stage migration after injection ceases. In this section, we will therefore perform a simple 'sensitivity analysis' that will tell us something of how the different geological parameters impact the flow responses discussed in the previous section. The five geological parameters impact the flow responses to different degrees; some parameters are more influential during injection, others take effect when the migration starts after injection has ceased, and some are influential both during injection and migration. Comparing the relative impact of the different parameters will indicate which of the parameters are most important to represent accurately when modeling a specific aquifer of the type considered herein.

To quantify the relative impact of each geological parameter, we will define normalized sensitivities that measure how much each of the basic flow responses discussed in the previous section change due to a unit change in a normalized geological parameter. We emphasize that these sensitivities cannot be interpreted as gradients in the strict mathematical sense. We will use barriers as an example to explain the analysis. There are three levels of barriers: low, medium and high. Suppose that we want to calculate the sensitivity of the number of plumes with respect to the level of coverage for the barrier sheets. We do this in two steps: first we average the number of plumes for cases of the same level of barriers. Having three levels of barrier, this results in three averaged plume numbers corresponding to each level of barriers. In the next step, we fit a line through these three points and calculate the

slope of this line, which thus represents how the number of plumes increases if the barrier parameter increases one level. For other parameters like fault and lobosity, we follow the same procedure. We use three levels for each parameter and fit a trend through these three points. For example, the first level of fault criteria relates to unfaulted cases, the second relates to open faults, and the third represents cases with closed faults.

Figure 12 shows the sensitivity for three different flow responses. In the upper row, we see that during injection the average aquifer pressure is most influenced by aggradation, while at the end of simulation the most influential parameter is the fault specification. The lack of good vertical communication for low aggradation angles means that the CO₂ is confined to the lower (poor quality) layers and relatively high pressures must be imposed to inject the required amount of CO₂ into the aquifer. For higher angles, the CO₂ can flow more easily upward through channels with higher permeabilities and less pressure support is required. Hence, the negative sensitivity. After the injection ceases, the dominating force is gravity, the main flow direction is vertical, and the pressure is now mostly affected by faults. If the faults are closed, they will prevent the release of pressure through the open boundaries. We also observe that the effect of progradation switches from positive to negative after the injection is stopped: Injecting in the up-dip direction is easier than injecting down-dip, while a down-dip deposition opens up more conductive medium in front of the plume as it migrates toward the crest.

The second row in Figure 12 shows the sensitivity in the number of CO₂ plumes. During injection, the barrier coverage is the most influential parameter, because mud-draped surfaces enhance the lateral flow and force the plume to split rather than migrating toward and accumulating at the crest. Aggradation has a similar effect: the lower the angle is, the more the injected CO₂ spreads out laterally. At the end of simulation, progradation and aggradation are the dominant effects. In particular, higher aggradation angle improves the segregation across layers and thus increases the splitting of plumes through heterogeneities. The impact of the faults is more significant than the figure shows: open faults contribute to split plumes, while the unfaulted cases and the cases with closed faults introduce a small number of plumes. In average, the positive and negative contributions cancel out to almost zero. Finally, the bottom row in Figure 12 reports sensitivities for the total residual volume. Here, aggradation is the most influential parameter during injection and faults the most important parameter during the migration phase.

The discussion is based on the overall trend averaged over all realizations and one should therefore be careful to draw general conclusions. For example, pressure sensitivity values with respect to progradation dip direction are based on only two points: the average over all cases with up-dip progradation and the average over all cases with down-dip direction. In Figure 12, we see that the progradation sensitivity changes polarity from the end of injection to the end of simulation. Squeezing the information of about 80 cases in one point makes it more difficult to make a general conclusion from this result. Figure 13 shows that some cases do not follow the trend shown in Figure 12. While there is a slight increase in the average level of pressure values from Figure 13a to Figure 13b, the average pressure level is decreasing when we compare Figure 13c to Figure 13d.

Similar analyzes have been conducted for other flow responses as well. Altogether, our sensitivity study shows that aggradation is the parameter that has most impact on the flow responses we have studied. Aggradation has either the largest or the second largest sensitivity during both injection and migration for almost all responses. The faulting has the second highest impact. Mostly effected by closed fault, the fault parameter influences the storage capacity and the extent to which a CO₂ plume accumulates under the caprock. Barriers play a dominating role for the splitting of plumes during injection, whereas the progradation affects the gravity segregation through conductive channels during the migration phase and the volume available to flow in the dip direction. Finally, lobosity has small impact compared to the other parameters and can therefore likely be ignored for the fluid responses considered above. However, lobosity has a considerable effect on the lateral movement and splitting of plumes during the migration period and may therefore have a more significant impact on the estimates of point leakage.

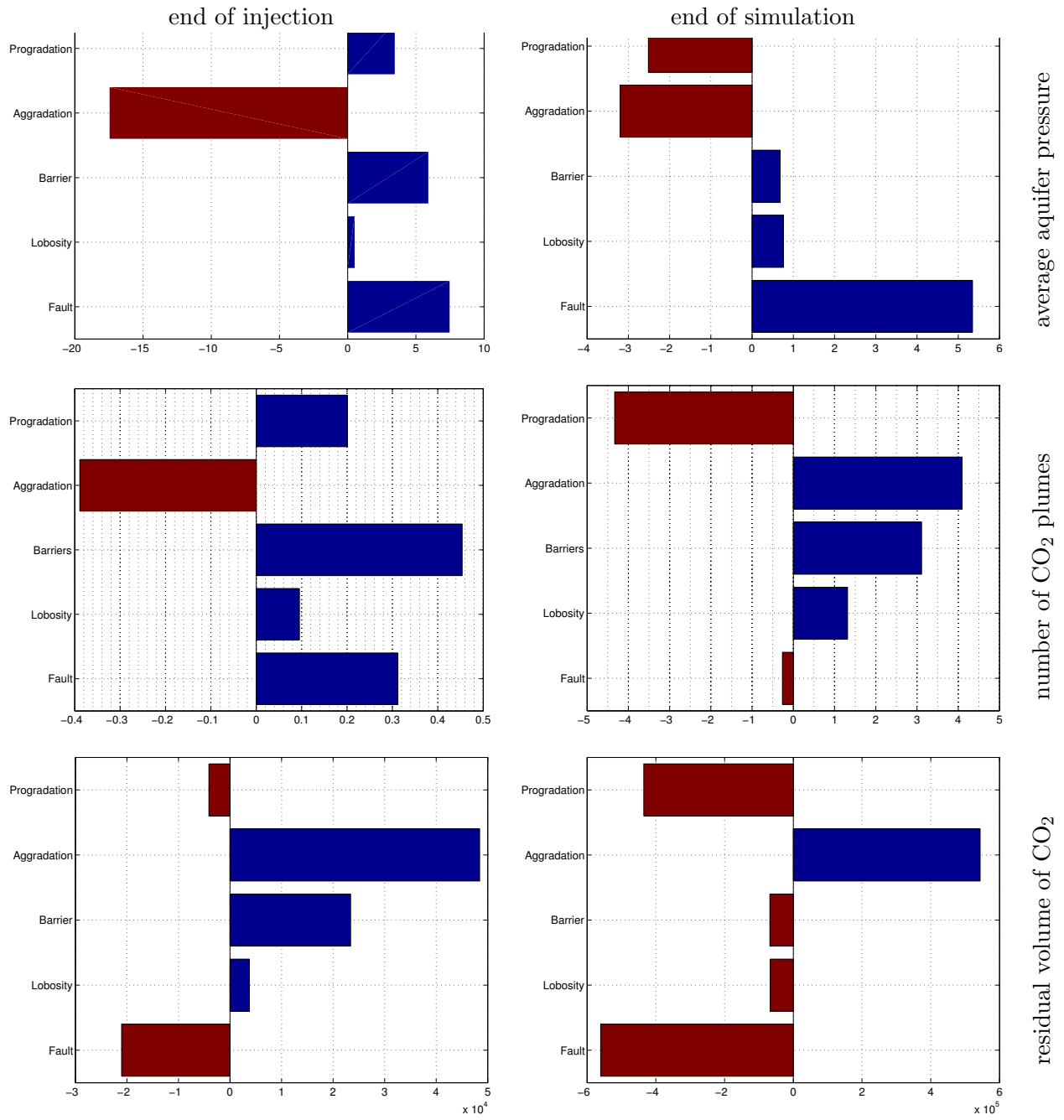
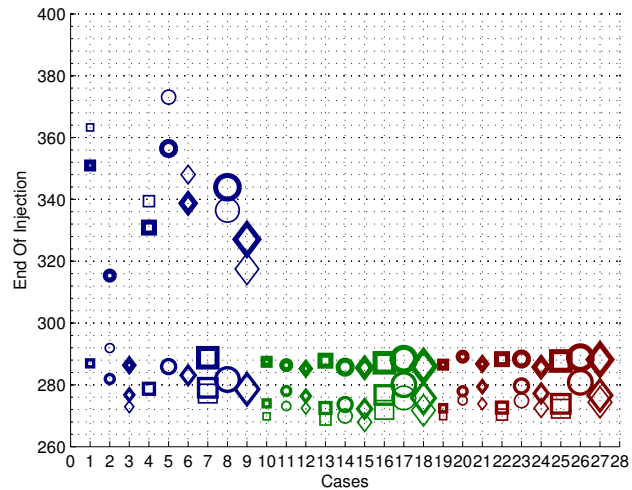
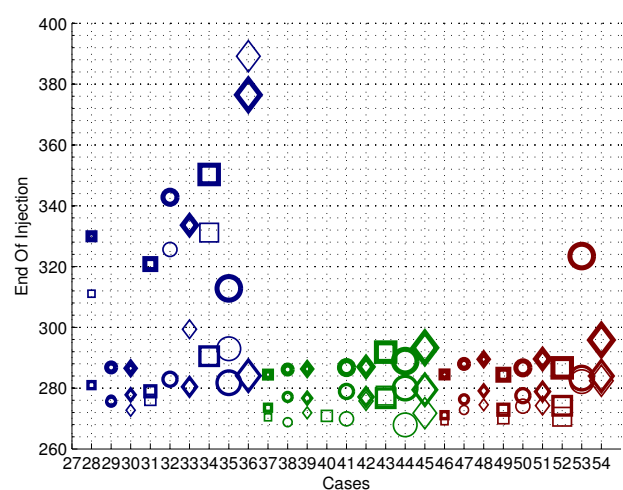


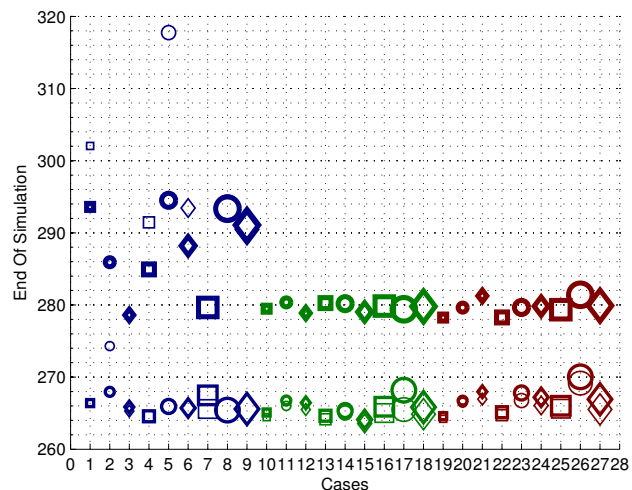
Figure 12: Sensitivities to different geological parameters at end of injection and end of simulation for the average aquifer pressure, number of CO₂ plumes, and residual volume of CO₂.



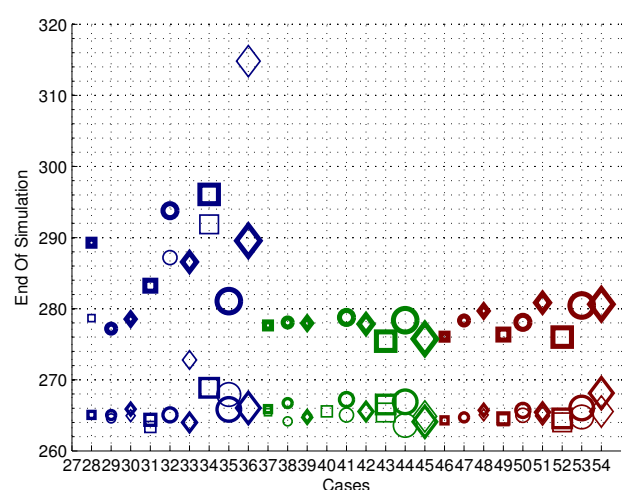
(a) Up-dip progradation, end of injection.



(b) Down-dip progradation, end of injection.



(c) Up-dip progradation, end of simulation.



(d): Down-dip progradation, end of simulation.

Figure 13: Effect of progradation on the pressure response.

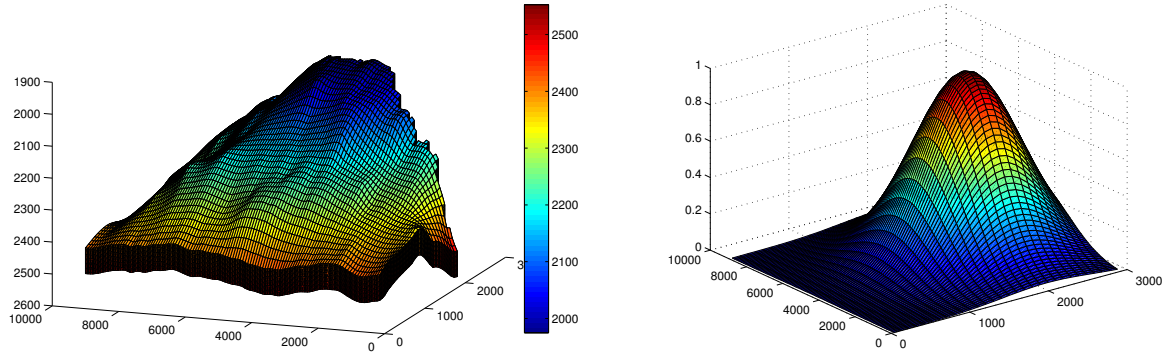


Figure 14: The left plot shows a sample grid geometry with depth values shown in meters. The right plot shows the Gaussian probability distribution for point leakage through the caprock. The distribution is centered at a point on the crest which is in the same slice as the injection point.

5 Risk for Point-Leakage

The capillary-sealing potential of the caprock is typically expressed in terms of the maximum over-pressure that the brine-saturated caprock can sustain, and leakage will only take place if the pressure of the CO₂ column exceeds this capillary entry pressure. The entry pressure is controlled by the interfacial tension between brine and CO₂, the water-wettability of caprock minerals, and the pore size distribution within the caprock [35, 15, 16, 14, 48]. The water-wettability is altered in the presence of CO₂ under pressure conditions that are typical for a storage site. Pore-size distribution is due to depositional factors.

The SAIGUP study does not supply any information about the caprock and its geomechanical properties (including breaches and other regions of “high permeability” that may form potential leakage paths). We are therefore only able to conduct a conceptual study of the risk associated with point leakage through imperfections in the caprock. To this end, we assume that each point on the top surface has a prescribed probability for being a leakage point. In lack of any useful information, we will simply assume that the probability for point leakage follows a standard 2D Gaussian distribution centered at a given point on the crest, see Figure 14. This is physically unrealistic, but simple to treat mathematically. Moreover, we will also disregard the effects of capillary entry pressure and wettability alterations, which contribute to reduce potential leakage rates, and simply assume that all mobile CO₂ (except for the residual portion) will escape through the caprock if a plume comes in contact with a leakage point. We have seen above that the heterogeneity and tilt of the medium will cause the injected CO₂ to be distributed under the caprock as a number of plumes with variable sizes. For each cell along the top surface, we now define the risk as the probability of point leakage weighted by the volume of the CO₂ plume that the cell is part of. We then sum the values for all the topmost cells, normalize this sum, and use the resulting single number as a measure of leakage risk. The worst possible case would be if all the injected CO₂ volume forms a mobile plume that contacts every point along the top surface; this gives a risk value equal to one. For all reasonable cases, however, the risk value will be less than one because not all of the CO₂ will be mobile (because of residual trapping and loss of volumes across the open boundaries), because the mobile volume may form more than one plume, or because not all the mobile volume has reached the top due to reduced vertical mobility.

Figure 15 shows the resulting leakage risk for all cases at the end of simulation computed using linear relative permeabilities. Similarly, the left plot in Figure 16 shows how the risk changes during the seventy year period from the end of injection to the end of simulation, whereas the right plot shows a cross-plot of the leakage risk versus the total volume of mobile CO₂. The plots lead to the rather obvious conclusion that improved vertical connection will increase the risk of mobile CO₂ migrating upward to connect a potential breach in the caprock, and hence that there is a positive correlation between the volume of mobile CO₂ in the system and leakage risk. However, we also observe that there are cases which have zero risk for leakage through the caprock. These are cases with low aggradation, for which the flow stays in the injected layers and moves laterally toward the open boundaries, resulting in a low amount of mobile CO₂ in the system. Furthermore, these cases have

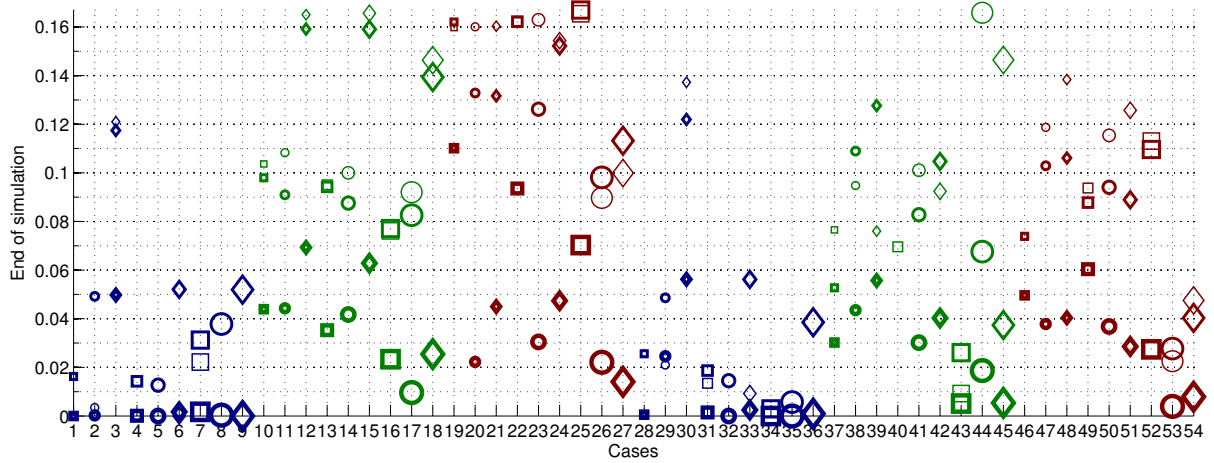


Figure 15: Leakage risk at the end of simulation for linear relative permeabilities.

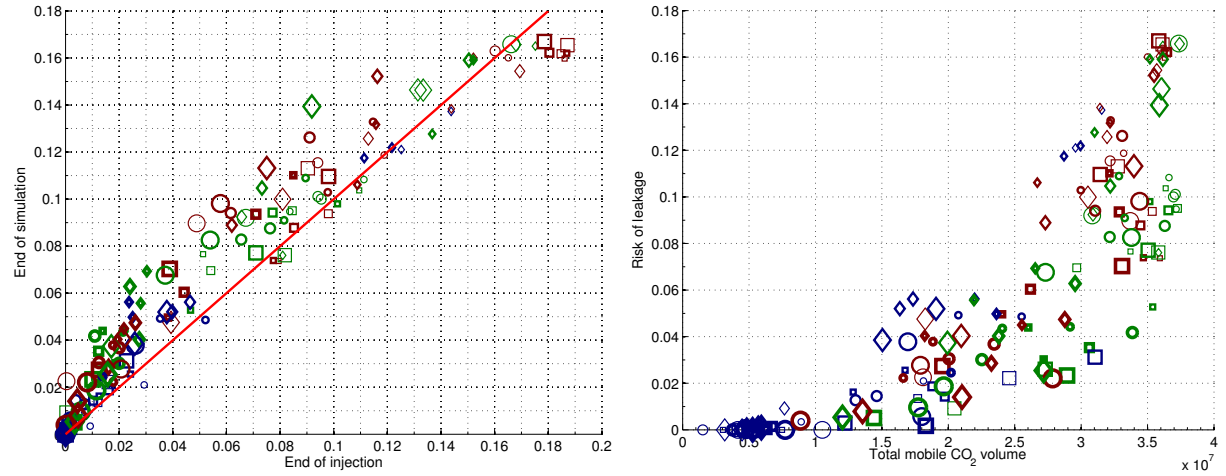


Figure 16: The left plot shows a cross-plot of leakage risk for linear relative permeability function. The right plot shows mobile CO_2 volume versus leakage risk at the end of simulation.

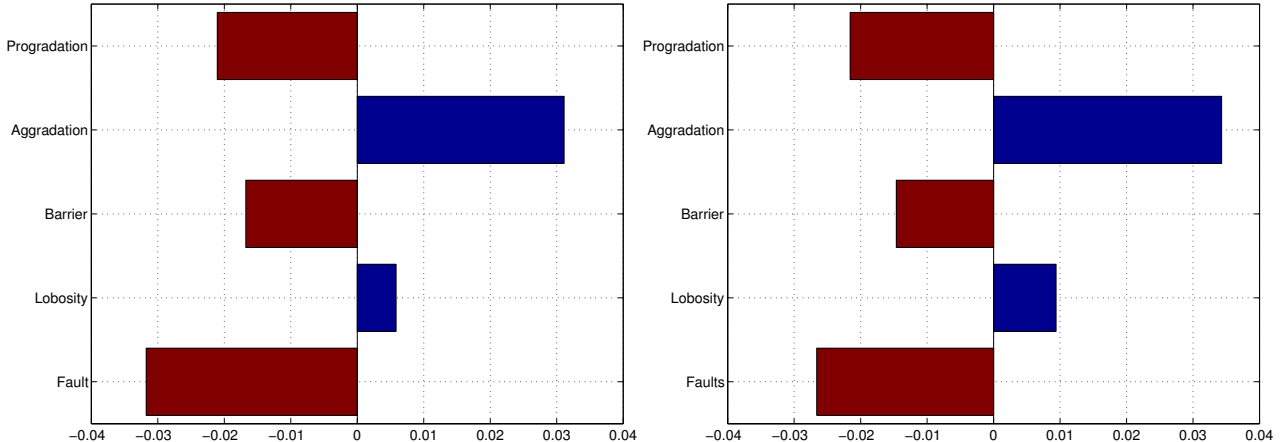


Figure 17: Sensitivity of the leakage risk with respect to the five geological parameters at the end of injection (left) and at the end of simulation (right).

(almost) no cross-layered CO₂ movement, which means that (almost) no CO₂ reaches the top surface. In other words, the low-aggradation cases, which have seemed to be unfavorable in our discussion in the previous two sections because of high injection pressure, larger lateral spread, and loss of volumes through the open boundaries, here appear as the most favorable with respect to potential leakage through imperfections the caprock.

Figure 17 shows sensitivities for the leakage risk. Because the total injected volume of CO₂ corresponds to 20% of the available pore volume, a major plume will in a majority of the cases have migrated to the crest of the reservoir already during the injection phase. Hence, the leakage-risk sensitivity shows almost the same profile at the end of injection and the end of simulation. This can also be observed in Figure 16. The sensitivity is slightly less during injection compared to at the end of simulation, because more CO₂ will accumulated below the caprock at the end of simulation. This overtakes the effect of the reduction in mobile volumes because of residual trapping and the increase in the number of plumes at end of simulation, which both result in less risk of leakage.

Once again, aggradation angle and fault criteria are the two most influential parameters. Increasing the aggradation angle improves the vertical communication and contributes to enhance the formation of CO₂ plumes below the caprock. Closed faults limit the movement of the plume and result in less accumulation below the caprock, whereas open faults generally increase the upward migration of plumes.

6 Conclusions

We have presented a study of how various geological parameters influence the injection and early-stage migration of CO₂ in progradational shallow-marine systems. One hundred and sixty equally probable realizations were considered and several flow responses related to storage capacity and risk of point leakage were calculated at the end of injection and after seventy years of gravity-dominated plume migration based on simulations using both linear and nonlinear relative permeabilities. We believe that linear permeabilities are a good starting point when studying the long-term impact of geological heterogeneities when this impact can be considered a first-order effect as herein. Flow predictions using nonlinear relative permeabilities are more sensitive to vertical grid resolution and can lead to severe under-prediction of gravity segregation effects in low-saturation regions if this resolution is not chosen sufficiently fine (see e.g., [36]). A more comprehensive study should therefore investigate the need for vertical (and lateral) grid refinement as in [52]. Vertical grid refinement will typically result in a CO₂ plume that is thinner vertically and has a much larger areal extent. If the segregated plume only fills the upper fraction of the grid cells, the movement of the plume will effectively be governed by linear permeabilities if capillary effects are small. For these reasons, we have herein primarily used linear permeabilities, which give significantly higher wave speeds and lead to earlier accumulation of CO₂ under the caprock and hence provide more pessimistic estimates of the plume migration and the risk associated with point leakage after a prescribed number of years than what is obtained by (possibly under-resolved) simulations with nonlinear relative permeabilities.

Altogether, we have demonstrated and discussed how the heterogeneity induced by different geological parameters give large variations in flow responses. Each geological parameter will influence the flow behavior and can result in local/global pressure build-up or pressure drop, enhance the flow direction, hinder the flow in the medium, or lead to loss of injected volumes over the open boundaries, and may induce different effects during the injection and plume migration. Specifically, we have demonstrated how variation in aggradation angle, fault criteria, and progradation direction significantly change the flow direction within the medium and hence impact the residual trapping and formation of movable CO₂ plumes under the caprock. Barriers are important during injection and must be modeled more carefully if the study focuses on injection operations. The large variations observed herein—e.g., for the reservoir pressure—are of course somewhat exaggerated by the fact that we consider a fixed injection point without regard to whether this point is favorable or not for each specific model realization. Despite this, we believe that our study shows that geological heterogeneity has a major impact on the injection and formation of a CO₂ plume and the subsequent early-stage migration of this plume. Any predictive study should therefore incorporate a realistic and detailed description of the geological heterogeneity as well as estimates of geological uncertainty to provide reliable forecasts of operational risks and the long-term fate of injected CO₂.

References

- [1] M. Akbarabadi and M. Piri. Relative permeability hysteresis and capillary trapping characteristics of supercritical CO₂/brine systems: an experimental study at reservoir conditions. *Advances in Water Resources*, 2012.
- [2] I. Akervoll and P. Bergmo. A study of Johansen formation located offshore Mongstad as a candidate for permanent CO₂ storage. In *European Conference on CCS Research, Development and Demonstration. 10–11 February 2009, Oslo, Norway*, 2009.
- [3] M. Ashraf. Impact of geological heterogeneity on early-stage CO₂ plume migration: pressure sensitivity study. *Submitted*, 2013.
- [4] B. Bennion and S. Bachu. Drainage and imbibition relative permeability relationships for supercritical CO₂/brine and H₂S/brine systems in intergranular sandstone, carbonate, shale, and anhydrite rocks. *SPE Reservoir Evaluation & Engineering*, 11(3):487–496, 2008.
- [5] B. Bennion and S. Bachu. Drainage and imbibition CO₂/brine relative permeability curves at reservoir conditions for carbonate formations, spe 134028. In *SPE Annual technical conference and exhibition, Florence, Italy, Society of Petroleum Engineers*, 2010.
- [6] P. E. S. Bergmo, E. G. Lindeberg, F. Riis, and W. T. Johansen. Exploring geological storage sites for CO₂ from Norwegian gas power plants: Johansen formation. *Energy Procedia*, 1(1):2945–2952, 2009.
- [7] M. Bickle, A. Chadwick, H. E. Huppert, M. Hallworth, and S. Lyle. Modelling carbon dioxide accumulation at Sleipner: Implications for underground carbon storage. *Earth and Planetary Science Letters*, 255:164–176, 2007.
- [8] R. Bissell, D. Vasco, M. Atbi, M. Hamdani, M. Okwelegbe, and M. Goldwater. A full field simulation of the In Salah gas production and {CO₂} storage project using a coupled geo-mechanical and thermal fluid flow simulator. *Energy Procedia*, 4(0):3290–3297, 2011.
- [9] F. C. Boait, N. J. White, M. J. Bickle, R. A. Chadwick, J. A. Neufeld, and H. E. Huppert. Spatial and temporal evolution of injected CO₂ at the Sleipner Field, North Sea. *Journal of Geophysical Research: Solid Earth*, 117(B3), 2012.
- [10] M. Burton, N. Kumar, and S. L. Bryant. CO₂ injectivity into brine aquifers: Why relative permeability matters as much as absolute permeability. *Energy Procedia*, 1(1):3091–3098, 2009.
- [11] A. Cavanagh and P. Ringrose. Simulation of {CO₂} distribution at the In Salah storage site using high-resolution field-scale models. *Energy Procedia*, 4(0):3730 – 3737, 2011.
- [12] R. A. Chadwick and D. J. Noy. History-matching flow simulations and time-lapse seismic data from the Sleipner CO₂ plume. *Geological Society, London, Petroleum Geology Conference series*, 7:1171–1182, 2010.
- [13] R. A. Chadwick, P. Zweigel, U. Gregersen, G. A. Kirby, S. Holloway, and P. N. Johannessen. Geological reservoir characterization of a CO₂ storage site: The Utsira Sand, Sleipner, northern North Sea. *Energy*, 29(9–10):1371–1381, 2004. 6th International Conference on Greenhouse Gas Control Technologies.
- [14] C. Chalbaud, M. Robin, J. Lombard, F. Martin, P. Eggermann, and H. Bertin. Interfacial tension measurements and wettability evaluation for geological CO₂ storage. *Advances in Water Resources*, 32(1):98–109, 2009.
- [15] P. Chiquet, D. Broseta, and S. Thibault. Capillary alteration of shaly caprocks by carbon dioxide. In *SPE Europec/EAGE Annual Conference*, 2005.
- [16] P. Chiquet, D. Broseta, and S. Thibault. Wettability alteration of caprock minerals by carbon dioxide. *Geofluids*, 7(2):112–122, 2007.

- [17] H. Class et al. A benchmark study on problems related to CO₂ storage in geologic formations. *Comput. Geosci.*, 13(4):409–434, 2009.
- [18] P. J. Cook, A. Rigg, and J. Bradshaw. Putting it back where it came from: Is geological disposal of carbon dioxide an option for Australia. *Australian Petroleum Production and Exploration Association Journal*, 1, 2000.
- [19] G. T. Eigestad, H. K. Dahle, B. Hellevang, F. Riis, W. T. Johansen, and E. Øian. Geological modeling and simulation of CO₂ injection in the Johansen formation. *Computational Geosciences*, 13(4):435–450, 2009.
- [20] M. Flett, R. Gurton, and G. Weir. Heterogeneous saline formations for carbon dioxide disposal: Impact of varying heterogeneity on containment and trapping. *Journal of Petroleum Science and Engineering*, 57(1-2):106–118, 2007.
- [21] A. Förster, B. Norden, K. Zinck-Jørgensen, P. Frykman, J. Kulenkampff, E. Spangenberg, J. Erzinger, M. Zimmer, J. Kopp, G. Borm, et al. Baseline characterization of the CO₂SINK geological storage site at Ketzin, Germany. *Environmental Geosciences*, 13(3):145–161, 2006.
- [22] O. Gharbi, B. Bijeljic, E. Boek, and M. J. Blunt. Changes in pore structure and connectivity induced by CO₂ injection in carbonates: a combined pore-scale approach. In *Proceedings of the international conference on greenhouse gas technologies (GHGT)*, volume 11, 2012.
- [23] A. L. Goater, B. Bijeljic, and M. J. Blunt. Dipping open aquifers—the effect of top-surface topography and heterogeneity on CO₂ storage efficiency. *International Journal of Greenhouse Gas Control*, 17:318–331, 2013.
- [24] W. D. Gunter, S. Bachu, and S. Benson. The role of hydrogeological and geochemical trapping in sedimentary basins for secure geological storage of carbon dioxide. *Geological Society, London, Special Publications*, 233(1):129–145, 2004.
- [25] B. Hitchon. *Aquifer disposal of carbon dioxide: hydrodynamic and mineral trapping: proof of concept*. Geoscience Pub., 1996.
- [26] S. D. Hovorka, C. Doughty, S. M. Benson, K. Pruess, and P. R. Knox. The impact of geological heterogeneity on CO₂ storage in brine formations: a case study from the Texas Gulf Coast. *Geological Society, London, Special Publications*, 233(1):147–163, 2004.
- [27] J. A. Howell, A. Skorstad, A. MacDonald, A. Fordham, S. Flint, B. Fjellvoll, and T. Manzocchi. Sedimentological parameterization of shallow-marine reservoirs. *Petroleum Geoscience*, 14(1):17–34, 2008.
- [28] R. Juanes, E. J. Spiteri, F. M. Orr Jr, and M. J. Blunt. Impact of relative permeability hysteresis on geological CO₂ storage. *Water Resources Research*, 42:W12418, 2006.
- [29] T. Kempka, H. Class, U.-J. Görke, B. Norden, O. Kolditz, M. Kühn, L. Walter, W. Wang, and B. Zehner. A dynamic flow simulation code intercomparison based on the revised static model of the Ketzin pilot site. *Energy Procedia*, 40(0):418–427, 2013.
- [30] T. Kempka, M. Kühn, H. Class, P. Frykman, A. Kopp, C. Nielsen, and P. Probst. Modelling of {CO₂} arrival time at Ketzin—Part I. *International Journal of Greenhouse Gas Control*, 4(6):1007–1015, 2010.
- [31] A. Kopp, H. Class, and R. Helmig. Investigations on CO₂ storage capacity in saline aquifers: Part 1. dimensional analysis of flow processes and reservoir characteristics. *International Journal of Greenhouse Gas Control*, 3(3):263–276, 2009.
- [32] S. Krevor, R. Pini, L. Zuo, and S. M. Benson. Relative permeability and trapping of CO₂ and water in sandstone rocks at reservoir conditions. *Water Resources Research*, 48(2), 2012.
- [33] H. Law and S. Bachu. Hydrological and numerical analysis of CO₂ disposal in deep aquifer systems in the Alberta sedimentary basin. *Ener. Convers. Mgmt*, 37(6-8):1167–1174, 1996.

- [34] U. Lengler, M. D. Lucia, and M. Kühn. The impact of heterogeneity on the distribution of co₂: Numerical simulation of {CO₂} storage at Ketzin. *International Journal of Greenhouse Gas Control*, 4(6):1016–1025, 2010.
- [35] S. Li, M. Dong, Z. Li, S. Huang, H. Qing, and E. Nickel. Gas breakthrough pressure for hydrocarbon reservoir seal rocks: implications for the security of long-term CO₂ storage in the weyburn field. *Geofluids*, 5(4):326–334, 2005.
- [36] I. S. Ligaarden and H. M. Nilsen. Numerical aspects of using vertical equilibrium models for simulating CO₂ sequestration. In *Proceedings of ECMOR XII–12th European Conference on the Mathematics of Oil Recovery*, Oxford, UK, 6–9 September 2010. EAGE.
- [37] E. Lindeberg. Escape of CO₂ from aquifers. *Energy Conversion and Management*, 38:S235–S240, 1997.
- [38] T. Manzocchi, J. N. Carter, A. Skorstad, B. Fjellvoll, K. Stephen, J. A. Howell, J. D. Matthews, J. J. Walsh, M. Nepveu, C. Bos, J. Cole, P. Egberts, S. Flint, C. Hern, L. Holden, H. Hovland, H. Jackson, O. Kolbjørnsen, A. MacDonald, P. A. R. Nell, K. Onyeagoro, J. Strand, A. R. Syversveen, A. Tchistiakov, C. Yang, G. Yielding, and R. W. Zimmerman. Sensitivity of the impact of geological uncertainty on production from faulted and unfaulted shallow-marine oil reservoirs: objectives and methods. *Petroleum Geoscience*, 14(1):3–15, 2008.
- [39] J. D. Matthews, J. N. Carter, K. D. Stephen, R. W. Zimmerman, A. Skorstad, T. Manzocchi, and J. A. Howell. Assessing the effect of geological uncertainty on recovery estimates in shallow-marine reservoirs: the application of reservoir engineering to the saigup project. *Petroleum Geoscience*, 14(1):35–44, 2008.
- [40] H. M. Nilsen, P. A. Herrera, M. Ashraf, I. Ligaarden, M. Iding, C. Hermanrud, K.-A. Lie, J. M. Nordbotten, H. K. Dahle, and E. Keilegavlen. Field-case simulation of CO₂-plume migration using vertical-equilibrium models. *Energy Procedia*, 4(0):3801–3808, 2011. 10th International Conference on Greenhouse Gas Control Technologies.
- [41] H. M. Nilsen, A. R. Syversveen, K.-A. Lie, J. Tveranger, and J. M. Nordbotten. Impact of top-surface morphology on CO₂ storage capacity. *International Journal of Greenhouse Gas Control*, 11(0):221–235, 2012.
- [42] J. M. Nordbotten and M. A. Celia. *Geological Storage of CO₂: Modeling Approaches for Large-Scale Simulation*. John Wiley & Sons, Hoboken, New Jersey, 2012.
- [43] J. M. Nordbotten, D. Kavetski, M. A. Celia, and S. Bachu. A semi-analytical model estimating leakage associated with CO₂ storage in large-scale multi-layered geological systems with multiple leaky wells. *Under Review at: Environmental Science and Technology*, 2008.
- [44] E.-O. I. Obi and M. J. Blunt. Streamline-based simulation of carbon dioxide storage in a North Sea aquifer. *Water Resources Research*, 42(3), 2006.
- [45] Y. Pamukcu, S. Hurter, P. Frykman, and F. Moeller. Dynamic simulation and history matching at Ketzin (CO₂SINK). *Energy Procedia*, 4(0):4433–4441, 2011.
- [46] Y. Pamukcu, S. Hurter, L. Jammes, D. Vu-Hoang, and L. Pekot. Characterizing and predicting short term performance for the In Salah Krechba field {CCS} joint industry project. *Energy Procedia*, 4(0):3371–3378, 2011.
- [47] J.-C. Perrin and S. Benson. An experimental study on the influence of sub-core scale heterogeneities on CO₂ distribution in reservoir rocks. *Transport in porous media*, 82(1):93–109, 2010.
- [48] H. Shao, J. R. Ray, and Y.-S. Jun. Dissolution and precipitation of clay minerals under geo-logic CO₂ sequestration conditions: CO₂–brine–phlogopite interactions. *Environmental science & technology*, 44(15):5999–6005, 2010.

- [49] E. Spiteri, R. Juanes, M. Blunt, and F. Orr. Relative-permeability hysteresis: Trapping models and application to geological CO₂ sequestration. In *SPE Annual Technical Conference and Exhibition*, 2005.
- [50] A. R. Syversveen, H. M. Nilsen, K.-A. Lie, J. Tveranger, and P. Abrahamsen. A study on how top-surface morphology influences the storage capacity of CO₂ in saline aquifers. In P. Abrahamsen, R. Hauge, and O. Kolbjørnsen, editors, *Geostatistics Oslo 2012*, volume 17 of *Quantitative Geology and Geostatistics*, pages 481–492. Springer Netherlands, 2012.
- [51] L. Van der Meer. The CO₂ storage efficiency of aquifers. *Energy Conversion and Management*, 36(6):513–518, 1995.
- [52] L. Wei and F. Saaf. Estimate co2 storage capacity of the johansen formation: numerical investigations beyond the benchmarking exercise. *Computational Geosciences*, 13(4):451–467, 2009.
- [53] L. Zuo, S. Krevor, R. W. Falta, and S. M. Benson. An experimental study of CO₂ exsolution and relative permeability measurements during CO₂ saturated water depressurization. *Transport in porous media*, 91(2):459–478, 2012.